J. Indian Inst. Sci.
A Multidisciplinary Reviews Journal
ISSN: 0970-4140 Coden-JIISAD

REVIEW ARTICLE

Validation of Chemical Bonding by Charge-Density Descriptors: The Current Scenario

*Venkatesha R. Hathwar**

Abstract | Electron-density distribution influences the chemical and physical properties of a material. Modern experimental and theoretical charge-density methods have become reliable in determining the nature of chemical bonding. Latest developments in the field of X-ray sources, detector technologies, and new analytical descriptors have helped it evolve over the years as a dynamic area of advanced crystallography. This review provides a short introduction to charge-density methods and highlights recent experimental results to understand the chemical concepts and material properties better. Potential applications of charge-density analysis and possible directions are discussed.

1 Introduction

X-ray diffraction (XRD) is one of the best known methods for precise and accurate determination of atomic and molecular structures of crystalline materials. Since the discovery of XRD by a crystal, its importance has been realized in all branches of modern science and technology. A precise knowledge of atomic positions and thus of the geometrical structure of the material is prerequisites to understand and predict the chemical and physical properties of any material. Ever since "forbidden" 222 reflection was first measured in diamond by Bragg during the 1920s,[1] the focus of crystallography research has shifted to extract finer details of chemical bonding in a molecule. The introduction of atom-centered multipole models (MM) in the 1970s[2–4] has effectively incorporated bonding density. MM has incorporated aspherical features of atomic density resulting from chemical interactions and lone pairs through a precise measurement of electron density (ED) through high-resolution X-ray diffraction data. Furthermore, topological properties of ED can be extracted from multipolar density using Bader's Quantum Theory of Atoms in Molecules (QTAIM).[5] It allows the quantitative evaluation of bonding features and, thus, its correlation with chemical reactivity of the molecule. Over the last decade, the field of charge-density (CD) analysis has grown rapidly due to significant advances in hardware and detector technologies in combination with the availability of brighter X-ray sources, such as microfocus X-ray tubes for laboratory X-ray diffractometers and synchrotron radiations.[6, 7] The rapid increase in computing power has also played an important role in the success of new technologies, especially related to quick acquisition and processing of huge quantity of measured data. These developments have helped CD analysis to become a reliable experimental method for crystalline compounds. It was successfully applied to many complex systems, for example, inorganic extended structures,[8] biological systems,[9] and even to powder X-ray diffraction (PXRD) data[7] to expand its potential application to a wider range.

X-ray data requirements for CD modeling are quite different from routine crystal structure determination, the primary requirement being the availability of high-quality single crystals without any twinning and disorder. In addition, CD analysis demands high-resolution X-ray data, normally up to $(\sin\theta/\lambda)_{max}$ >1.1 Å^{-1}, measured with high accuracy and precision for better deconvolution of thermal motion and bonding features. Both accuracy and precision in data measurement are essential as the valence electrons contribute to a small portion of intensity compared to the total number of electrons. They provide all the chemically most important information. Indeed, recent advanced detectors for X-rays, such as charge-coupled device

*Correspondence:
hathwar.rama.fw@u.tsukuba.ac.jp;
mudradivenky@gmail.com
Division of Physics,
Faculty of Pure
and Applied Sciences,
University of Tsukuba,
Tsukuba 305-8571, Japan

(CCD), complementary metal-oxide semiconductor (CMOS), imaging plate (IP) and new-generation hybrid pixel detectors (XPAD, Pilatus and Medipix) and realization of intense monochromatic X-ray sources via rotating anodes, and microfocus tubes with multilayer mirror optics provide good-quality X-ray data with high signal-to-noise ratio. In addition, it is often necessary to cool the crystal using either nitrogen or helium cryogenics to obtain enough intensity at higher angles and to minimize thermal diffuse scattering (TDS). In this context, synchrotron radiation has become an ideal probe for CD experiments[7] and it offers many advantages over a laboratory X-ray diffractometer, namely, tunable photon energy, higher intensity, and shorter data-acquisition time. Higher intensity allows use of smaller crystals for data collection, thus minimizing crystal absorption and extinction problems. Furthermore, a reliable synchrotron data and considerable improvements in the data-treatment software for synchrotron data have enabled CD method applicable to more complex and challenging systems.

Thermal diffuse scattering: is inelastic scattering where the incident X-rays on the specimen excite thermal vibrations (lattice vibrations) of atoms in the specimen and scattered in a diffuse manner.

Synchrotron: is an extremely powerful source of X-rays where accelerated electrons emit energy at the X-ray wavelength while changing the direction in the circular path.

Numerous reviews[7, 10–15] highlight the importance of CD analysis in the understanding of bonding interactions in a variety of chemical and biological systems. It is beneficial to refer some important textbooks on the topic for a detailed description of the methodology[16] and related theoretical background.[5, 17] Recent developments in the area of CD and its applications are included in new textbooks, namely, *Modern charge density analysis*,[18] edited by C. Gatti and P. Macchi and *Electron density and chemical bonding* I and II,[19] edited by D. Stalke. In the present review, the current scenario in the field of CD analysis to study organic compounds, metal–organic compounds, extended inorganic compounds, CD studies using synchrotron powder X-ray diffraction (SPXRD), and CD analysis under external perturbations have been critically examined based on contemporary experimental results published since 2012.

2 Historical Perspective and Charge-Density Models

The impact of X-rays on the development of crystallography was not imagined when W. C. Röntgen discovered them in 1895. The first XRD experiment was performed in 1912 by M. von Laue in Munich by exposing several crystals (copper sulfate pentahydrate and zinc sulphide, in particular) to X-rays.[20] He used a piece of photographic film to record the diffraction X-ray pattern. A simplified explanation for Laue's experiment was formulated by W. L. Bragg and W. H. Bragg by considering the interaction between X-rays and an electron cloud of atoms, which later came to be known as the Bragg's law. Indeed, they solved the crystal structure of several inorganic crystals, e.g., NaCl, ZnS, FeS_2, and diamond. However, the main obstacle in solving the crystal structure of organic compounds was unknown phasing information from scattered X-rays during diffraction experiments. Subsequent developments, such as the Patterson function[21] by L. Patterson in 1930s, the direct method[22] by J. Karle and H. Hauptman in the 1950s using the Sayre Equations,[23] came handy in the determination of small-molecule structures.

In the XRD experiment, the ED in the unit cell is obtained through an inverse Fourier series summation over measured all Bragg structure factors (F_{hkl}):

$$\rho(\mathbf{r}) = \frac{1}{V}\sum_{h,k,l} F_{hkl} e^{-2\pi i(hx+ky+lz)} \quad (1)$$

where x, y, and z are fractional coordinates of atoms, such that $\mathbf{r} = x\mathbf{a} + y\mathbf{b} + z\mathbf{c}$. V, and hkl are the unit cell volume and Miller indices, respectively. Once the physical model for the crystal structure of a material is determined from X-ray data, both the atomic position and thermal parameter of the atom allow refinement through least-squares procedure to create an agreement between observed and calculated structure factors. An obvious way to expedite the model-building process would be to exploit the power of the computer. Several structure solution and refinement programs have been developed to accurately determine the crystal structure. In this context, the independent atom model (IAM) has very successfully determined the crystal structure of a crystalline material accurately. It works on the assumption that atomic electron density is well described by the spherically averaged density of the isolated atom. Hence, the ED in the molecule is described as a superposition of isolated spherical densities ρ^0 of isolated atoms k centered at R_k. The atomic density of the molecule in the IAM is expressed as

$$\rho_{\mathrm{IAM}}(\mathbf{r}) = \sum_k \rho_k^0(\mathbf{r} - \mathbf{R}_k). \quad (2)$$

The success of IAM has been confirmed by a large number of crystal structure determinations, which are now readily available in the Cambridge Structure Database (CSD) and Inorganic Crystal Structure Database (ICSD). The aspherical features of ED in the bonding region are

completely neglected in the IAM. Hence, quantitative description of chemical bonding is limited to determining the bond lengths and bond angles. To overcome deficiencies of IAM, the first attempt was to project the ED,$\rho(\mathbf{r})$ into atomic-like terms by combining radial coefficients and harmonic functions.[24] Aspherical modeling of ED was systematically developed with a significant improvement in theory to include chemical-bonding features. In the early 70s, many atom-centered deformation models were proposed for the determination of electron density distribution (EDD) from the XRD data (see below).

In 1967, Dawson[24] proposed an atom-centered deformation model based on radial functions combined with appropriate Kubic harmonics, which was later extended by Kurki-Suonio[25] with more flexible radial functions. Hirshfeld[26] had suggested a deformation model using angular functions of $\cos^n$ type, which are linear combinations of spherical harmonics to express the deformed ED. The deformation function on each atomic center in the Hirshfeld's model is expressed as

$$\rho_{i,n} = \sum_{i,n} P_{i,n} N_m \mathbf{r}^n \exp(-\alpha_i \mathbf{r}_i) cos^n \theta_k \tag{3}$$

where $P_{i,n}$ is an adjustable population parameter, $\mathbf{r}_i$ is the distance from atomic center i, α_i is a parameter that governs the radial breadth of the deformation function on each type of atom, N_m is a normalization factor, and θ is the angle between a radius vector $\mathbf{r}$ and a specific polar axis k.

In 1976, Stewart[2] suggested the ED model, where the pseudo-atom density is expressed as a spherical core density together with a multipolar valence density as given by

$$\rho_i(\mathbf{r}) = \rho_{\text{core}} + \sum_{l,m} P_{l,m} R_l(\mathbf{r}) Y_{l,m\pm}(\theta,\phi) \tag{4}$$

where $R_l(\mathbf{r})$ is the radial part of density and expressed in terms of Slater-type functions as

$$R_l(\mathbf{r}) = N\mathbf{r}^n \exp(-\zeta \mathbf{r}) \tag{5}$$

where N is the normalization constant, and ζ is the energy-optimized single Slater exponent for the electron sub-shells of isolated atoms. The angular part of the density is represented by spherical harmonic functions, $Y_{l,m\pm}(\theta,\phi)$ in Eq. (4). Multipole projection of aspherical density, as described by Stewart, was incorporated in the Hansen and Coppens (HC) model development with modifications.

In another approach, Coppens et al.[27] proposed a simple modification to IAM by including valence charge transfer between bonding atoms through either expansion or contraction of the valence shell. This model is well known in the CD community as kappa formalism or radial refinement. In this model, the scattering contribution of valence electrons is separated from that of inner shells to consider the adjustment of population and radial dependence of the valence shell. The basic assumption of this model is that the electrons of core shells are unperturbed and the atomic density is expressed as

$$\rho_{\text{atom}}(\mathbf{r}) = \rho_{\text{c}}(\mathbf{r}) + P_{\text{v}}^3 \rho_{\text{v}}(\kappa \mathbf{r}) \tag{6}$$

where P_{v} is the valence shell population parameter and κ represents the radial parameter which allows contraction or expansion of the valence shell. The parameter κ scales with the radial coordinate $\mathbf{r}$. If $\kappa > 1$, then the same density is obtained at a smaller $\mathbf{r}$ value, and consequently, the valence shell is contracted. On the other hand, the valence shell expands for $\kappa < 1$. This model allows calculating the magnitude and direction of dipole moments and net atomic charges. The results obtained from kappa formalism are in good agreement with the experimental and theoretically calculated values.[27] However, this model had failed to describe the aspherical distribution of ED between the atoms. The complete description of the ED of atoms in the molecule involves accounting for both spherical contraction/expansion of valence shell and aspherical features of bonding density based on the nature of hybridization of the participating atoms.

In 1978, Hansen and Coppens[4] suggested the formalism of MM by combining the kappa model features with spherical harmonic angular functions and Slater-type radial functions for aspherical density. The atomic density in the HC multipole formalism[4] is defined as

$$\rho_{\text{atom}}(\boldsymbol{r}) = P_{\text{c}}\rho_{\text{c}}(\boldsymbol{r}) + P_{\text{v}}\kappa^3 \rho_{\text{v}}(\kappa \mathbf{r}) + \sum_{l=0}^{l_{\max}} \kappa'^3 R_l\left(\kappa' \mathbf{r}\right) \sum_{m=0}^{l} P_{lm\pm} Y_{lm\pm}(\theta,\phi) \tag{7}$$

where ρ_{c} and ρ_{v} represent the Hartree–Fock spherical core and valence electron densities, respectively, P_{c} and P_{v} are the core and valence shell populations, respectively, and P_{v} gives an estimation of the net atomic charge by $q = N_{\text{v}} - P_{\text{v}}$, where N_{v} is the number of valence electrons in a free neutral atom. The terms, $Y_{lm\pm}$, $P_{\text{lm}\pm,}$ and $R_{l,}$ represent real spherical harmonic functions of order l and m corresponding to the orientation of l, the multipolar population parameters, and the Slater-type radial function, respectively. The coefficients κ and κ' describe the

contraction–expansion of spherical and multipolar valence densities, respectively. The radial function of deformation density in the form of normalized Slater functions is given as

$$R_l(\mathbf{r}) = \kappa'^3 \frac{\zeta^{nl+3}}{(n_l+2)!}\left(\kappa'\mathbf{r}\right)^{\mathrm{n}(l)} \exp(-\kappa'\zeta_l\mathbf{r}) \qquad (8)$$

where coefficients $n_l \geq 1$ to satisfy Poisson's electrostatic equation as pointed out by Stewart[28] and ζ represents the energy-optimized single Slater exponent for the electron sub-shells of isolated atoms.

Multipole modeling of high-resolution X-ray data will efficiently deconvolute the thermal motion and the ED. The quality and correctness of MM are examined by the Hirshfeld rigid-body test,[29] residual density or probability density function (pdf),[30] and fractal dimension distribution of residual density.[31] Once a reliable MM is obtained, the bonding features are directly analyzed through static deformation density map, which shows the density deformation with respect to promolecular density. The static deformation density is described as

Residual density: is the difference between the observed and the modeled ED.

$$\Delta\rho_{\mathrm{static}}(\mathbf{r}) = \rho_{\mathrm{MM}} - \rho_{\mathrm{IAM}} \qquad (9)$$

where ρ_{MM} and ρ_{IAM} are, respectively, the thermally averaged density obtained from MM and spherically averaged density from promolecule.

Another important issue in MM is the treatment of H-atoms during multipole refinement as they are crucial for a correct estimation of HB strengths. Obtaining the correct position and accurate description of atomic displacement parameters (ADPs) for the H-atom from X-ray diffraction data is always problematic, but they are necessary for an unbiased MM and error-free ED properties involving H-atoms. Especially, the strength of HBs and their relation with chemical reactivity of the molecule depend on the accurate description of H-atoms. In this context, combined X-ray and neutron-diffraction measurements, and subsequent MM are the most accurate but often are beset with difficulties due to inadequate experimental facilities, long data-acquisition times, and large crystal size requirement. In such cases, the *SHADE2* web server[32] and Hirshfeld atom refinement (HAR)[33] provide ADPs of H-atoms for multipolar modeling of X-ray data. Another method, the X-ray-constrained wavefunction (XCW),[34] has become a promising alternative to MM refinement for CD analysis using both theoretical calculation and experimental data. In XCW, theoretically obtained wavefunction is allowed to deform during the refinement process, so that the calculated X-ray structure factors best match the experimental ones. The 'experimental wavefunction' obtained is thus used for the estimation of physical properties of the material. In many CD studies, the ED results are comparable to MM using the XCW.[35]

Multipolar expansion of the ED using HC formalism is the most applicable and accurate. Afterwards, a large number of least-squares refinement software packages have been developed by several groups to model X-ray data based on the HC model, for example, *MoPro*[36] and *XD*.[37] Now, the analysis of EDD from experimental X-ray data has become very popular and has reached a stage of complete maturity with a wide range of applications in the fields of physics, chemistry, materials science and biology.

3 Topology of Electron Density and Bonding Descriptors

Static deformation density obtained from multipolar modeling does not include any thermal smearing effects, so it can be used to check chemical concepts, such as bonding density and lone-pair regions. Furthermore, static deformation density maps help judge the correct deconvolution of the experimental model by comparing multipole density with the theoretically derived density from the wavefunction. However, the ED alone does not explain the nature of chemical bonding in molecules, especially the mechanism of electron sharing between atoms. Thus, experimental ED has to be subjected to Bader's QTAIM[5] analysis to extract bonding information from MM density. Essentially, it provides a quantitative link between total ED and the bonding features of the molecule, bypassing the wavefunction in the analysis. According to a unique partitioning scheme of the QTAIM, the total density of the molecule is divided into open subsystems referred to as atomic basins, a physically meaningful separation of the molecule into its atoms. It allows determining many properties from individual basins, e.g., net atomic charges, atomic volumes, and electrostatic moments. In addition, this includes the analysis of ED at critical points (CPs) $\rho(\mathbf{r}_{\mathrm{cp}})$, where the gradient of the ED vanishes, $(\nabla\rho(\mathbf{r}_{\mathrm{cp}}) = 0)$. The CP corresponds to the local minima, local maxima, and saddle points of the EDD. The second derivative of the ED given by the Hessian matrix is known as the Laplacian, $\nabla^2\rho(\mathbf{r}_{\mathrm{cp}}) = (\lambda_1 + \lambda_2 + \lambda_3)$, where λ_i defines the eigenvalues of the Hessian matrix. The rank and signature of the Hessian matrix classify the CPs into nuclear critical points (NCP), bond critical

Atomic basin: is defined as a region of space in which all the electrons are bound to the nucleus.

points (BCP), ring critical points (RCP), and cage critical points (CCP) with (3, −3), (3, −1), (3, +1), and (3, +3) labels, respectively. The Laplacian also recovers the shell structure of the atom to reveal a local accumulation/depletion of the ED. If the ED is locally concentrated, then $\nabla^2\rho(\mathbf{r}_{cp}) < 0$ and $\nabla^2\rho(\mathbf{r}_{cp}) > 0$ for locally depleted ED at a given point in space. In the case of shared interactions, the value of $\rho(\mathbf{r}_{cp})$ is relatively high and $\nabla^2\rho(\mathbf{r}_{cp}) < 0$, whereas for closed shell interactions, the value of $\rho(\mathbf{r}_{cp})$ is small and $\nabla^2\rho(\mathbf{r}_{cp}) > 0$. The line of the highest ED between two atoms is defined as the 'bond path' and it can deviate from linearity based on the distribution of ED. Indeed, the bond path, the electron density, and Laplacian values at CPs together represent the topology of the EDD of the bond in a given molecule. Hence, QTAIM provides a methodology for the quantitative understanding of chemical bonding between two interacting atoms in a molecule that gained a lot of importance in the evaluation of nature of interactions between two atoms.

In recent years, many additional descriptors for chemical bonding have been developed for a better understanding of the bonding mechanism. For example, electron localization function (ELF),[38] Source Function (SF) analysis,[39] electron localization and delocalization indices,[40,41] non-covalent interactions (NCI) descriptor,[42] distributed atomic polarizability,[43] and nucleus-independent chemical shifts (NICS)[44] are widely used to unravel sensitive aspects of bonding, such as covalency, iconicity, aromaticity, conjugation, hydrogen bonds (HBs), and van der Waals interactions of molecules.

ELF was originally formulated by Becke and Edgecombe[38] to measure electron localization. It has been extensively used for evaluating the concept of electron-pair localization in numerous molecules and solids. It lies on the conditional same-spin pair probability $[D_\sigma(\mathbf{r})]$ scaled by homogeneous electron gas kinetic energy density $[D_\sigma^0(\mathbf{r})]$ and is defined as

$$\mathrm{ELF} = \eta(\mathbf{r}) = \frac{1}{1 + x_\sigma(\mathbf{r})^2} \tag{10}$$

and

$$\chi_\sigma(\mathbf{r}) = \frac{D_\sigma(\mathbf{r})}{D_\sigma^0(\mathbf{r})} = \frac{\tau_\sigma(\mathbf{r}) - \frac{1}{4}\frac{|\nabla\rho_\sigma(\mathbf{r})|^2}{\rho_\sigma(\mathbf{r})}}{\frac{3}{5}(6\pi^2)^{2/3}\rho_\sigma^{5/3}(\mathbf{r})} \tag{11}$$

has helped in understanding the concept of electron-pair localization in numerous molecules and solids, where $\rho_\sigma(\mathbf{r})$ is the σ-spin density and $\tau_\sigma(\mathbf{r})$ is the spin contribution to positive definite kinetic energy density. ELF ranges from 0 to 1, where 1 indicates a high probability of finding electron localization.

According to SF analysis,[39] the ED, $\rho(\mathbf{r})$, at any given point $\mathbf{r}$ within a molecule is determined by contributions from a local source $\mathrm{LS}(\mathbf{r},\mathbf{r}')$ operating at all other points $\mathbf{r}'$ and is given by

$$\rho(\mathbf{r}) = \int \mathrm{LS}\left(\mathbf{r},\mathbf{r}'\right)\,\mathrm{d}\mathbf{r}' \tag{12}$$

$$\text{where, } \mathrm{LS}\left(\mathbf{r},\mathbf{r}'\right) = \frac{-\nabla^2\rho(\boldsymbol{r})}{4\pi\left|\mathbf{r}-\mathbf{r}'\right|}. \tag{13}$$

Bond path: is a line of maximal ED connecting two atomic domains via a BCP.

Hence, the ED at $\mathbf{r}$ is related to local behavior in terms of the Laplacian weighted by the influence function, $4\pi\left|\mathbf{r}-\mathbf{r}'\right|^{-1}$. It quantifies the influence of all other parts of a system to the local property or chemical behavior of the system.

Intermolecular interactions in molecular crystals can be quantitatively evaluated by the analysis of atomic polarizabilities, in particular, their deformation in the crystal. For this purpose, Krawczuk et al.[45] developed the program PolaBer to estimate distributed atomic polarizabilities using a partitioning of ED through QTAIM. The molecular polarizability tensor can be decomposed into atomic polarizability tensors and they are computed by numerical derivatives of atomic dipole moments with respect to external electric field. The atomic polarizability is given by

$$\alpha_{ij}(\Omega) = \frac{\mu_i^{E_j}(\Omega) - \mu_i^0(\Omega)}{E_j} \tag{14}$$

where $\mu_i^{E_j}(\Omega)$ is the atomic dipolar component of the atomic basin Ω along the i direction with a given electric field (0 or ε) in the j direction. Atomic polarizabilities in a molecule are visualized as ellipsoids, whose size is proportional to total atomic polarizability and the ellipsoid axes represent the anisotropy of polarizability due to perturbations, such as intermolecular interactions.

Similarly, one more versatile tool, the NCI descriptor based on reduced electron density gradient (RDG), was introduced by Johnson et al.[42] for visualizing regions of space involved in either attractive or repulsive interactions. The RDG $[s(r)]$ is a dimensionless quantity and expressed as

$$s(\mathbf{r}) = \frac{|\nabla\rho(\mathbf{r})|}{2(3\pi)^{1/3}\rho(\mathbf{r})^{4/3}}. \tag{15}$$

The NCIs are characterized by low ED and RDG values. The mapping of the quantity, $\mathrm{sign}\lambda_2\rho(\mathbf{r})$, on RDG isosurfaces can distinguish

stabilizing [sign$\lambda_2\rho(\mathbf{r}) < 0$] and destabilizing [sign$\lambda_2\rho(\mathbf{r}) > 0$] interactions in the crystal, where λ_2 is the second largest eigenvalue of the Hessian matrix. This method was later extended to experimental ED by Saleh et al.[46] by developing the NCImilano program. It is now further extended to obtain a relationship between stabilization energy and kinetic energy density integrated over volume bounded by RDG isosurfaces.[47]

4 Applications

4.1 Organic Compounds and Proteins

The σ-hole: is referred to the electron-deficient outer lobe of a half-filled *p* (or nearly *p*) orbital involved in forming a covalent bond.

The ability of the CD method to evaluate the nature of intra- and intermolecular interactions and the chemical reactivity in organic compounds has made it one of the best quantitative methods available in chemistry. Nowadays, experimental determination of the ED in organic crystals is well-established and high-quality accurate CD results are normally obtained if good-quality single crystals are accessible. The main advantage of organic compounds is that valence electrons constitute a significant portion of the scattering intensity compared to that of core electrons and they carry all relevant chemical-bonding information. In addition, extinction and absorption effects are either small or insignificant for organic crystals. Hence, a conventional laboratory diffractometer can provide high-quality X-ray data required for CD modeling. An easy access to high-resolution X-ray data on organic crystals has spurred a large number of CD studies on organic compounds.[18] Many such studies have focused on the quantitative evaluation of weak interactions, stability and reactivity of different polymorphic modifications, analysis of chemical reaction pathways, and binding of drug molecules to an active site of proteins.[18] In the study of intermolecular interactions, Koch and Popelier[48] proposed eight necessary criteria based on QTAIM to identify a 'true' HB from that of a van der Waals interaction. These criteria are widely used in many organic compounds and succeeded in evaluating the nature of HBs. Likewise, the concept of Source Function (SF) introduced by Bader and Gatti[39] has provided more detailed inputs on the nature of HBs based on values of atomic SF contributions to ED at the BCP of HBs.[49] In recent times, CD analysis of HBs has become a reliable method and experimental results are often very consistent with well-established theoretical calculations. In the experimental CD model, even small values of ED (~0.01 eÅ^{-3}) at the BCP of intermolecular interactions are reproduced with high accuracy when compared with theoretically obtained values.[50] In the study of halogen bonding, the anisotropic distribution of ED around the halogen atom (σ-hole formation) in molecular compounds has been experimentally validated in many CD studies.[51–53] Deformation density and Laplacian maps, individual components of total interaction energy, have shown the dominant electrostatic nature of these interactions. However, interactions involving 'organic fluorine' are under debate on their stabilizing role in crystal packing.[54] Recently, type II C–F···F–C and C–F···S–C interactions involving fluorine atom in pentafluorophenyl 2,2′-bithiazole have been established as a realistic '*σ*-hole' interaction.[55] Both experimental and theoretical CD analyses[56, 57] demonstrate 'σ-hole' formation on fluorine atom in different chemical environments. A new bonding, known as 'carbon bonding',[58] has been proposed in methanol–water complex by theoretical calculations, where the carbon atom acts as an electrophilic site which can non-covalently bond with a nucleophilic atom. It is confirmed by experimental ED study in dimethylammonium 4-hydroxybenzoate,[59] where static deformation density and electrostatic potential maps show the 'σ-hole' formation on the carbon atom of $-CH_3$ moiety. In recent years, the concept of 'σ-hole' is extended to chalcogen bonding[60] and pnicogen bonding[61] in organic compounds. In an interesting CD study of Fmoc-Leu-ψ[CH_2NCS],[62] both 'σ-holes' and 'π-holes' have been simultaneously observed on the S atom and the C = N bond, respectively. For the first time, experimental evidence has been obtained by the CD analysis for simultaneous formation of 'σ-holes' and 'π-holes' in the molecule and they result in weak but highly directional and stabilizing N=C=S···N=C=S interactions in the crystal structure.

The organic semiconductor rubrene[63] and its oxidized form, rubreneendoperoxide,[64] were studied to correlate the ED and derived topological properties with their physical properties. The presence of electronic delocalization of π-density on the conjugated teracene backbone of the rubrene molecule and of π···π stacking interactions of distance 3.706(1) Å in solid state was experimentally confirmed by the CD study. These two factors are responsible for the observed high mobility of charges in rubrene. Furthermore, rubreneendoperoxide exhibits an 'O–O' charge-shift bonding (CSB) in the molecule, which is actively investigated in chemistry as a third chemical-bonding scenario in addition to known, classical covalent and ionic bonding. A fluctuating electron-pair density between two bonded

atoms plays an important role in determining the CSB. It is characterized by large covalent-ionic resonance interaction energy and depleted charge densities between bonded atoms as seen in F–F bonding. This has been further supported by electron localizability indicator (ELI-D), where it shows the loss of electronic localization in the O–O interatomic region by the lack of a significant bonding basin (Fig. 1).

The CD studies are also useful to shed light on the electronic differences between different polymorphic forms as well as their stability and reactivity in the solid state. The diuretic drug, acetazolamide, is evaluated to explore the unusual phenomenon of formation of a kinetic form over a thermodynamic form upon slow cooling of boiling aqueous solution.[65] The study establishes the change in hybridization on the N atom of the sulphonamide group, which is responsible for polymorphic modifications and this is known as "hybridization induced polymorphism". However, special care is required while interpreting the lattice energy results on different polymorphs based on MM density. In the study of polymorphic forms of sulfathiazole,[66] a model bias towards the estimation of lattice energy has been demonstrated, which might affect the ranking of polymorphic stability. It has been shown that the MM, particularly the treatment of the H-atom thermal motion, influences the lattice energy values obtained from experimental multipoles. Similarly, Spackman[67] in his study of atom···atom interactions highlighted an unreliable estimation of intermolecular interaction energies in molecular crystals by the Espinosa–Molins–Lecomte (EML) relationship.[68] EML energies of BCP properties, based on 166 atom–atom interactions in organic molecular crystals, significantly deviate from the benchmark values obtained from DFT calculations as well as energies estimated by the program *CrystalExplorer*.[69] In many cases, the EML energy provides wrong input on the energetic importance of specific interactions in crystal packing and their subsequent ranking in crystal structure.

Recent improvements to the HAR[33] method in the estimation of the H-atom position and its ADPs using routine X-ray data are promising. Its applicability has been successfully demonstrated even for strong O–H···O HBs (O···O distance is about 2.41 Å) in the L-phenylalaninium hydrogen maleate salt.[70] The X–H distances obtained and ADPs of individual atoms from the HAR method agree well with the values of neutron diffraction and the MM. HAR is further tested for a large number of X–H distances in different chemical environments of organic molecules and for H-atoms bonded to heavy transition metals in inorganic systems.[71]

The latest developments in synchrotron sources and data-analysis procedures have helped to determine high-quality crystal structures of proteins at subatomic resolution (~0.5 Å).[72] In many biological systems, even now, high-level computational calculations fail to provide fine structures of proteins due to the presence of large number of residues and bound water molecules. Hence, high-resolution data enable determine the fine structures of proteins, including H-atom positions, valence ED distribution, and orientation of bound water molecules. Recently, interesting CD studies have been reported on high-potential iron–sulfur protein (HiPIP) from the thermophilic purple bacterium *T. tepidum*[72] and cholesterol oxidase (ChOx).[73] The CD results provide the topological properties, atomic charges, and electrostatic properties of the active site to understand the relationship between

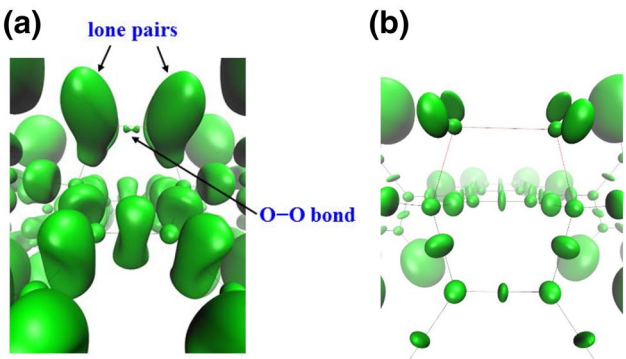

Figure 1: ELI-D isosurfaces depicting the O–O CSB bond with iso-values of (**a**) 1.35 and (**b**) 1.8. The O–O bond is represented by the *top horizontal line*. Reproduced with permission from[64] Copyright 2016: American Chemical Society.

structure and function of these proteins. Please refer to the dedicated review in this issue for an elaborate discussion on the CD methods related to biomolecules.

4.2 Metal–Organic and Inorganic Compounds

Another interesting class of compounds for the CD study is metal–organic compounds. A better understanding of the nature of metal–ligand interactions and metal–metal (M–M) bonding is essential for the analysis of their chemical, physical, and physiological properties. Recently, efforts were made to correlate the ED with magnetic properties of a material in molecular complexes. Overgaard et al.[74] reported the EDD in two analogous water-bridged dimetallic transition metal complexes, $[M_2(\mu\text{-}OH_2)\text{-}(^t BuCOO)_4(^t BuCOOH)_2(C_5H_5N)_2]$ (where M=Co and Ni) to derive a relationship between the ED and observed magnetic properties of the bulk sample. The absence of M–M BCP in both compounds confirms the absence of direct M–M interactions and this agrees well with magnetic and spectroscopic measurements. In another study, the relationship between the EDD and magnetic coupling constant has been derived for two metal–organic polymeric magnets, $Cu(pyz)(NO_3)_2$ and $[Cu(pyz)_2(NO_3)]NO_3{\cdot}H_2O$ (where pyz is pyrazine) by high-resolution XRD and the DFT calculations.[75] In this study, experimentally observed antiferromagnetic coupling constant is characterized by the inter-chain Cu–Cu superexchange interactions mediated by pyrazine-bridging ligands through an σ-exchange. The strength of the magnetic interactions does not depend on a tilt angle of the pyrazine ring with the plane defined by the $d_{x^2-y^2}$ magnetic orbital. In another interesting study, two types of Co atoms [low-spin Co(III) and high-spin Co(II)] in a mixed-valence tri-cobalt compound, $Co_3(\mu\text{-admtrz})_4(\mu\text{-}OH)_2(CN)_6{\cdot}2H_2O$[76] (admtrz = 3,5-dimethyl-4-amino-1,2,4-triazole) have been identified by respective d-orbital populations and integrated atomic charges. To obtain a precise description of the spin-dependent ED in magnetic compounds, a new software program *MOLLYNX*[77] was developed for the combined refinement of charge and spin densities. This unified model combines experimental high-resolution XRD and polarized neutron-diffraction (PND) data to provide charge and spin distribution of the material, respectively. A combined refinement was initially tested with a prototype bimetallic chain compound, $MnCu(pba)(H_2O)_3{\cdot}2H_2O$ [where pba is 1,3-propylene bis(oxamato)], using independent as well as combined analyses of charge and spin densities.[77] Excellent agreement exists between individual and joint refinements for static deformation density maps, and spin-density maps, including spin populations of atoms. Likewise, experimental determination of spin-resolved electron density distribution was made for the molecular complex, $Cu_2L_2(N_3)_2$ [where L is 1,1,1-trifluoro-7-((dimethylamino)-4-methyl-5-aza-3-hepten-2-onato)].[78] This study has provided experimental evidence for different contractions of spin-up and spin-down radial distributions for Cu atoms in the compound as theoretical calculation suggest.

In recent years, experimental and theoretical CD studies conducted on Ga-containing molecular compounds gave a reasonable ED model after using different radial scaling parameters for core electrons to describe the core density of Ga.[79], [80] The Laplacian distribution of the valence electrons and the ELI-D clearly demonstrates a charge localization region that points primarily away from the heterocycle in $[:Ga((C_6H_5N)_2CN(CH_3)_2)]$ and $[I_2Ga((C_6H_5N)_2CN(CH_3)_2)]$.[79] In addition, CD studies[80] confirm the ambiphilic reactivity of the Ga atom and its oxidation state of +1 in the compound $[GaN(C_6H_2[CHPh_2]_2(CH_3)\text{-}2,6,4)(Si(CH_3)_3)]$. Furthermore, ligand-induced charge concentrations (LICC) on the Ga atom suggest that the Ga–N bond in the compound could be characterized as an unusual metal–ligand dative bond with the roles of the metal and the ligand interchanged with respect to a "standard" metal–ligand interaction.

The M···H–C interactions in metal–organic complexes are an interesting area for the CD study to classify them as agostic, anagostic, and preagostic interactions and HBs due to their importance in many chemical reactions. Recently, the M–Si, M–H, and Si–H interactions were studied using CD analysis in the transition metal silane complexes, $Cp_2Ti(P(CH_3)_3)(SiH_2Ph_2)$ and $Cp_2Ti(P(CH_3)_3)(SiHCl_3)$.[81] The study aims to correlate the ED results with the metal-catalyzed Si–H bond activation process and the strength of the *M*–Si bond based on the extent of M → σ*(X–Si–H) π back donation. Indeed, non-vanishing Si–H interactions are clearly mirrored in charge-density studies to support the observation. Similarly, the square-planar $d^8\text{-}ML_4$ complexes, $Mo[Et_2B(pz)_2](\eta^3\text{-allyl})(CO)_2$ and $Ni[Et_2B(pz)_2]_2$ (where pz = pyrazolyl; allyl = H_2CCHCH_2) display M–H interactions and they were analyzed by combined experimental and theoretical CD studies to classify them as

either agostic or anagostic interactions.[82] Subtle but noticeable local Lewis acidic sites in axial direction in the Laplacian maps on the metal atom indicate a weak agostic nature for the M–H interaction. The results also demonstrate that the nature of weak agostic interactions is not correctly displayed in the ^{1}H NMR chemical shifts.

Low-valent silicon complexes are one of the most fascinating compounds to explore the nature of bonding using the CD model. Molecules containing a low-valent silicon atom in oxidation state zero with two lone pairs are known as silylones. To overcome the kinetic instability of these compounds, bulky groups are substituted to them. For experimental confirmation of low-valent silicon through CD analysis, high-resolution X-ray data were measured on $(cAAC)_2Si$, where cAAC is cyclic alkylamino carbenes.[83] Indeed, the Laplacian map shows two separated valence shell charge concentrations (VSCCs) in the non-bonding region of the central silicon atom. A singlet state for the carbene carbon has been displayed by a significant double-bond character in the nitrogen–carbene–carbon bond, which is necessary for the donor–acceptor bonding in silylones. Likewise, charge-density analysis on two isomers (ring and cage) of hexasilabenzene, $(TipSi)_6$[84] (where Tip is 2,4,6-triisopropylphenyl), established the aromaticity of the ring isomer and absence of an interstitial bond between Si^0 bridgehead atoms in the cage isomer. The formation of transannular VSCCs on opposite silicon atoms in the Laplacian map confirms the presence of two transannular bonds.

The literature has record of fewer CD studies on extended inorganic compounds. Absorption and extinction effects are severe in the experimental X-ray data due to heavy elements and formation of nearly perfect single crystals.[7] These systematic errors lead to significant problems in the modeling of ED and result in poor and unreliable experimental model. The latest improvements in synchrotron sources and hardware minimize these effects in addition to use of small crystals for the experiment. A recent CD study on a thermoelectric material, $CoSb_3$, illustrates the difficulties in the modeling of experimental data based on X-ray data sets measured by both conventional and different synchrotron sources.[85] This indicates that even with a small crystal (~10 μm), low temperature (10 K) and short wavelength (0.41 Å), obtaining an accurate ED model, is still a challenge for inorganic compounds. In $CoSb_3$, the net charges on the Co and Sb atoms are negative and positive, respectively, suggesting of a slightly polar interaction in the Co–Sb bond. The net charges on the Co and Sb atoms contradict a large part of the literature on thermoelectrics of skutterudites. In another study, the chemistry textbook concept of hypervalency in sulfate ions has been ruled out based on high-quality CD results in K_2SO_4.[86] The analyses of topological properties and Source Function (SF) demonstrate that the S–O bonds are highly polarized covalent bonds, where the 'single-bond' description prevails significantly over the 'double-bond' picture. The EDD in polymorphs of a photovoltaic material, FeS_2 (pyrite and marcasite), was determined to understand the differences in the nature of bonding between two polymorphs.[87] The significant difference between them is a more covalent S–S interaction and relatively weaker Fe–S interaction in pyrite compared to marcasite, which is directly reflected in their valence density distributions and corresponding d-orbital populations. In the CD study of a textbook example of Zintl phase, CaSi, the presence of predominant covalent Si–Si interactions experimentally confirms the Zintl–Klemm concept.[88] However, the Ca–Si bonds in the complex show a mixed ionic and covalent nature of interactions. This bonding in CaSi is attributed to highly polar Si → Ca σ-donation and somewhat weaker Si → Ca π-donation components. Furthermore, the partial covalent character of the Ca–Si bonds, as determined from net atomic charges, correlates well with the physical origin of the remarkable metallic properties of CaSi. The CD analysis of the ternary polyboride, $ScNiB_4$, brings out the differences between the interactions of Sc–B and Ni–B in heptagonal and pentagonal prismatic environments, respectively, of the crystal structure.[89] A local charge concentration (CC) resembling the angular shape of a d_{z^2}-type orbital has been observed for the Ni atom, whereas minute density accumulations are found in the Sc atom in $ScNiB_4$. These studies demonstrate that the CD method can reveal finer features of chemical bonding even of complex structural environments, which IAM cannot provide.

4.3 Charge-Density Analysis from SPXRD

As discussed, the majority of experimental ED studies in the literature belongs to single-crystal XRD using both laboratory and synchrotron X-ray sources.[7, 18] In recent years, however, SPXRD has emerged as an alternative probe for the study of EDD of crystalline materials, especially of extended inorganic materials with high-symmetry crystal structure and minimum peak overlap in powder pattern.[90] This is inherently

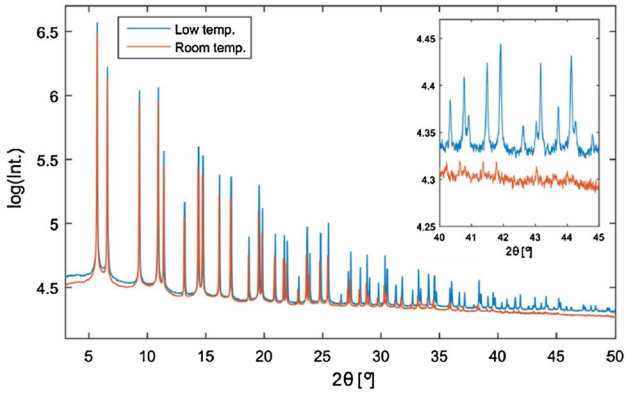

Figure 2: Comparison of powder-diffraction patterns of Cu at 293 K (no cooling) and 95 K (He cooled) measured up to $\sin\theta/\lambda = 2.2$ Å^{-1} in the all-in-vacuum diffractometer using Debye–Scherrer geometry and $\lambda = 0.20715$ Å. Adapted with permission from Ref.[92] Copyright 2016: International Union of Crystallography.

more challenging and complex compared to single-crystal data mainly due to the projection of three-dimensional (3D) reciprocal space into one dimension (1D). The advantages of SPXRD are the use of micron-sized powder including highly collimated and extremely intense high-energy incoming X-ray radiation from the diffraction experiment. These reduce absorption, anomalous scattering and extinction effects of the sample as well as instrumental broadening effects to the peak broadening of powder pattern. In addition, data collection is rapid in SPXRD compared with single-crystal XRD experiments and the whole PXRD is measured on a single scale. The single-crystal X-ray data are generally collected over different detector settings covering an entire reciprocal space, which often demands different exposure times with slightly different scale factors. Apart from many advantages over PXRD, the major challenges are the extraction of structure factors from powder pattern by correct subtraction of background and a proper estimation of reflection intensities from the peak overlap. These two processes directly influence the extracted peak intensities from PXRD. Hence, it is better to eliminate all possible contributors to the background intensity of the powder pattern to the extent possible. For any PXRD data, the fundamental lower limit to the background intensity corresponds to the Compton scattering from the sample and the total scattering from the container used to load the sample.[90] In recent years, B. Iversen and J. Als-Nielsen have pioneered the development of all-in-vacuum powder diffractometer to avoid all additional contributions to the background intensity of the powder pattern, especially originating from a scattering with the air.[91] The results from the all-in-vacuum powder diffractometer are encouraging and a significant increase is seen in the signal-to-noise ratio of the reflections along with background intensity close to its fundamental limit. It has further improved to cool the sample close to near-cryogenic temperature (95 K) during measurement using a jet of helium gas cooled by liquid nitrogen.[92] Superior-quality high-resolution PXRD data of copper [up to $\sin\theta/\lambda = 2.2$ Å^{-1}] have been measured using this setup without increasing the background intensity (Fig. 2). In addition, the quality of data has resulted in an extensive modeling of the thermal displacement parameters including weak anharmonic displacement features even at low temperature by the Gram–Charlier expansion of the temperature factor.[92]

The maximum entropy method (MEM) is traditionally employed to determine the EDD from SPXRD and extracted ED parameters are not influenced by the model bias in the MEM method. Nishibori et al.[93] have demonstrated that accurate structure factors required for reliable MEM calculations can be obtained from PXRD using the state-of-the-art third-generation synchrotron-radiation source and structure factors obtained are even comparable to the Pendellosung method. In their study, a benchmark SPRXD data on diamond with a resolution of $(\sin\theta/\lambda)_{max} = 1.45$ Å^{-1} were collected. The background intensity in the data was reduced by agglomerating the powder sample together by a tiny amount of glue instead of packing the sample in a glass capillary as commonly employed. The CD studies based on the MEM

method from SPXRD are routinely applied to a large number of extended inorganic structures and complex structural materials to explore their physical and chemical properties.[94] At the same time, the dynamic density obtained from the MEM method poses a challenge to interpret the results. However, recent methodological improvements related to dynamic density provide valuable semi-quantitative information on chemical bonding.[95] Svendsen et al.[96] systematically tested the multipole modeling method for CD studies using SPXRD while studying the EDD in diamond. The study demonstrates that the structure factor extraction based on the multipole model is the most accurate one. It further illustrates the radial defectiveness when a slightly wrong radial model (s^2p^2 instead of sp^3) was used for carbon in the multipole model, which results in a wrong thermal parameter. The correlation between the ED and thermal parameters has been shown even for a light atom, such as carbon. Furthermore, the deficiency of the standard HCMM [in Eq. (7)], while fitting high-resolution theoretical data is observed in the residual density maps. Based on this study, Fischer et al.[97] suggested the extended Hansen–Coppens (EHC) MM to overcome the deficiency in the standard HC model by abandoning the basic assumption of an inert core by parameterizing the inner shells of the atom. A modified expression for the EHC MM is given as

$$\rho_{\mathrm{EHC}}(r) = P_c\kappa_c^3\rho_c(\kappa_c r) + P_v\kappa_v^3\rho_v(\kappa_v r) + \sum_{l=0}^{l\max} \kappa_v'^3 R_l\left(\kappa_v' r\right) \sum_{m=0}^{l} P_{lm\pm} Y_{lm\pm}(\theta,\phi) \quad (16)$$

where κ_c and P_c are parameters to adjust for spherical deformation in the core region and other parameters are the same as in Eq. (7). The EHC model provides truly featureless residual density maps while dealing with ultra-high-resolution X-ray data and the core ED reveals how the innermost ED responds to the formation of chemical bonding. Using this upgraded CD model, a subtle contraction of the core shell ED (the deformation of the core ED) during the formation of covalent bonding has been demonstrated in the benchmark system, such as diamond, by both experimental and theoretical ED models.[90, 97] A systematic improvement in the residual density features with different ED models in the case of diamond is observed (Fig. 3). The experimental study has revealed that subtle ED features like core contraction phenomenon could be traced by ultra-high-resolution X-ray data and the topological values of the ED obtained are comparable with theoretical calculations. As an extension of core deformation studies, the EHC model has been applied to more complex systems, such as silicon[98] (where both anharmonicity and TDS are observed) and cubic boron nitride[99] (diatomic compound). Nishibori et al.[100] have applied a combination of MEM and HC multipole modeling in the study of EDD to $LiCoO_2$. Localized Co-3*d* electrons have been observed in deformation density from MEM. A large positive Laplacian value for the Co–O bond indicated that a slab of CoO_2 octahedra in $LiCoO_2$ is stabilized by ionic interactions. All these studies from PXRD show that multipole modeling can be applied to SPXRD data if all systematic errors can be avoided during the extraction of structure factors from the powder pattern. Even the standard HC modeling of the ED from SPXRD is a major advancement in the study of extended inorganic compounds.

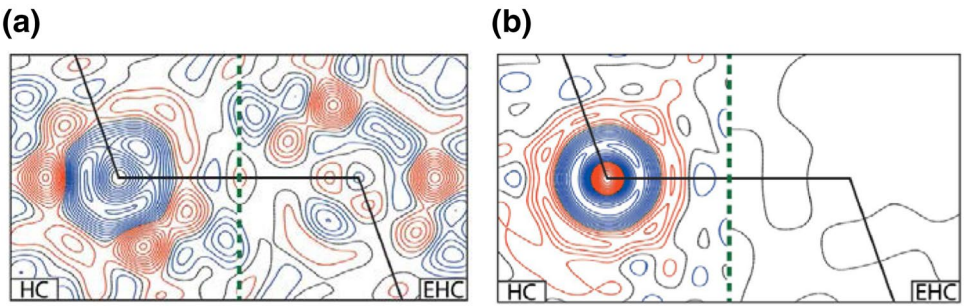

Figure 3: Residual densities of diamond from HC and EHC modeling using (**a**) experimental and (**b**) theoretical structure factors to a resolution of $\sin\theta/\lambda = 1.70$ Å^{-1}. Contours are drawn at 0.01 eÅ^{-3} intervals. Figures are adapted with permission from Ref.[7] and readers are advised to refer to Ref.[90] for complete details. Copyright 2016: International Union of Crystallography.

4.4 Charge-Density Studies Under External Perturbations

As discussed, the determination of EDD of crystalline materials at low temperature is now well established. At the same time, continuous efforts are on to increase the resolution and quality of X-ray data and to develop new characterization tools for bonding description to address new challenges. Among them, one of the tasks is to obtain the EDD of materials under external perturbations, such as pressure, light irradiation, external electric and magnetic fields. Good- quality data collection in these experiments is very difficult and demands an extensive experimental preparation and optimization. Often, high-resolution and good-quality data from these experiments can be obtained using synchrotron radiations only. To study the response of ED to the electric field, Hansen and coworkers[101] had developed a method and instrumentation to apply strong electric field to a crystal. They attempted to study the piezoelectric properties of α-quartz by accounting intensity variation using the least-squares refinement procedures in the *MOLLY-N* program though the results are very qualitative.[101] Recent diffraction studies under in situ electric filed using the XPAD hybrid pixel detector have shown promising results in this research area.[102] Likewise, for the first time, an excited-state EDD was determined on $Fe(phen)_2(NCS)_2$ (phen = 1, 10-phenanthroline) in high-spin metastable state using laser irradiation on the single crystal at the helium cryogenic temperature.[103] In this experiment, the quality of data was limited due to the high mosaicity of the crystal and incomplete photo-conversions by photo-irradiation. However, the results obtained from the photo-excitation CD experiment are promising and the 3d atomic orbital populations of the Fe atom corresponding to the metastable high-spin state ($t_{2g}^4e_g^2$ electron configuration) are experimentally determined.

Similarly, pressure is an efficient thermodynamic variable for generating new phases of a material, which will trigger new chemical reactions, conformational and structural transformations among different phases and polymerization.[104] Both chemical and physical properties of many materials under high pressures are still unknown and it is also difficult to predict pressure-generated reactions and transformations. Indeed, some chemical transformations under pressure are irreversible and they result in interesting material properties at ambient conditions. A major bottleneck to the ED determination from high-pressure X-ray diffraction (HPXRD) is the pressure apparatus (the Diamond Anvil Cell, DAC) used to generate pressure, which reduces drastically the resolution, completeness, and quality of measured data from the HP experiment.[104] Furthermore, unavoidable hindrances include high background intensity

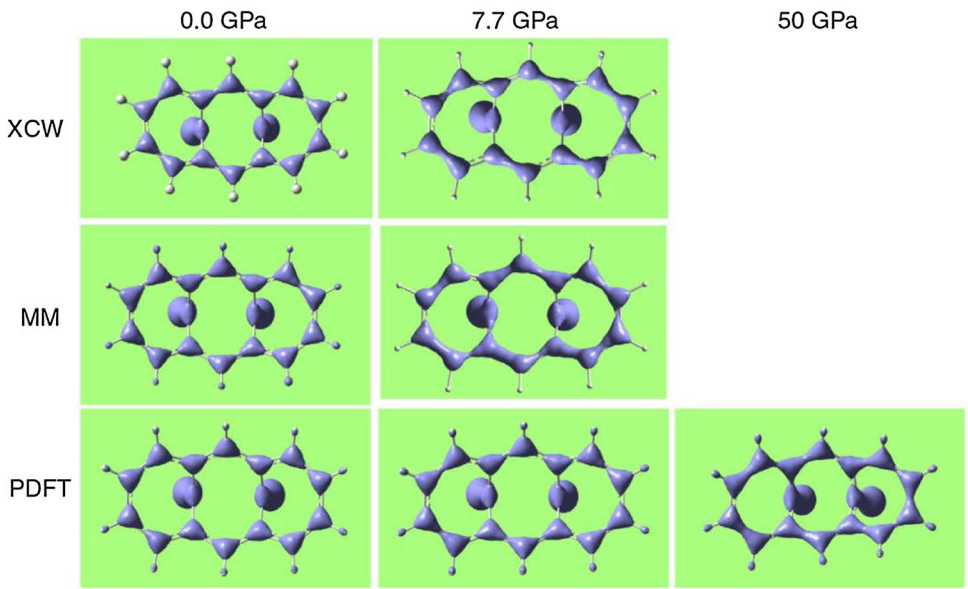

Figure 4: Demonstration of localization of the ED in one of the resonant configurations for BCA obtained from XCW, MM, and PDFT methods at higher pressure points. Adapted with permission from. [106] Copyright 2016: Nature Publishing Group.

coming from either a gasket or pressure-transmitting medium, limited opening angle of the DAC, the DAC absorption, and overlapped high-intense diamond scattering reflections. Several successful high-pressure CD studies on elemental solids, alloys, ionic solids, and extended structures have been reported from SPXRD using the MEM analysis. For example, material properties, such as charge transfer from the F atom to the K atom with increasing pressure in $KMnF_3$,[105] were established by HP experiment based on MEM analysis. While pushing the limits of high-pressure charge-density (HPCD) experiments, an experimental HPCD mapping on single crystals was obtained for an aromatic compound, syn-1,6:8,13-Biscarbonyl[14] annulene (BCA) by the MM.[106] In this interesting HPCD study, the localization of the ED in one of the resonant configurations for the aromatic compound, BCA, under high pressure has been experimentally determined. In addition, the experimental results are further supported by XCW analysis[34] and periodic density functional theory (PDFT) calculations to confirm the accuracy of the HPCD model (Fig. 4).

5 Charge-Density Research in India

X-ray crystallography has a strong tradition in India. However, CD analysis is practiced only by a limited number of research groups. It might be due to the fact that the determination of EDD demands very accurate and precise measurement of high-resolution X-ray data, which explicitly depends on good-quality single crystals and essential expertise. Long experimental durations, effort and cost of CD experiment act as constraints for its choice as an active research area for many researchers. The majority of experimental CD studies are from T.N. Guru Row and coworkers by the MM using high-resolution single-crystal XRD. It is mainly influenced by his association with P. Coppens during his postdoctoral research, where he was involved in the development of the kappa model.[27] After returning to India, his major contributions in the EDD include the determination of a lower limit for the C–H···O HB formation and 'region of overlap' between HBs and van der Waals interactions based on the Koch and Popelier's criteria.[107] Indeed, numerous intra- and intermolecular interactions are classified as strong HBs, weak HBs, and van der Waals interactions based on experimental and theoretical ED analyses.[108], [109] Similarly, halogen bonding,[110], [111] chalcogen bonding,[60] carbon bonding[59], and pnicogen bonding[61] have been quantitatively established using topological properties, electrostatic potentials, and estimated intermolecular interaction energies. The formation of a σ-hole on the donor atom (which drives all these bonding) has been experimentally confirmed through deformation density and Laplacian maps as well as in electrostatic potential isosurfaces. In another interesting study, a stabilizing cooperative interplay between σ-holes and π-holes has been experimentally validated for N=C=S···N=C=S intermolecular interactions in Fmoc-Leu-ψ[CH_2NCS], which is responsible for a reversible isomorphous phase transition upon cooling.[62] A collaboration between T. N. Guru Row and G. Desiraju at the Indian Institute of Science has resulted in a new charge-density databank, known as supramolecular synthon-based fragments approach (SBFA) for the transferability of multipole parameters utilizing modularity and robustness of supramolecular synthons.[112] This approach was initially tested for an O–H···O carboxylic acid dimer synthon and an N–H···O amide infinite chain synthon in the crystal structures. Later, the SBFA was extended for other weak interactions.[113] C. N. R. Rao and G. Kulkarni have carried out several experimental CD studies, for example, evaluation of polymorphism[114] and molecular properties of organic NLO materials.[115] Apart from experimental CD studies, theoretical aspects of the ED are being pursued by S. Gadre and coworkers. Their important contributions include estimation of molecular electrostatic potentials (MESP),[116] the study of lone pairs from the MESP,[117] and AIM in the momentum space by the Hirshfeld atomic partitioning scheme.[118] In addition, they have developed a software package *DAMQT*[119] for topological analysis and MESP. Presently, P. Munshi at Shiv Nadar University, Noida, D. Chopra at IISER, Bhopal, T. Thakur at the Central Drug Research Institute, Lucknow, and P. Kumaradhas at Periyar University, Salem, are actively pursuing charge-density research to explore material properties from EDD.

6 Conclusions and Outlook

As discussed earlier, CD studies on organic and metal–organic molecules are now well-established and CD experiments follow more or less well-established standard procedures. However, more experimental studies are needed in the case of extended materials, multipole modeling of SPXRD and the CD analysis under external perturbations, such as pressure and photo-irradiation. The experiments have many practical limitations and always pose new challenges for

both the experiment and data analysis. In this direction, the comparison of experimental results with reliable theoretical calculations provides many times a win–win situation for both experiment and theory. Furthermore, the XCW method has become encouraging as it combines both experimental and theoretical inputs. However, its further development for extended structures will provide necessary information while dealing with complex structures. In recent years, the use of synchrotron radiation has helped to improve the resolution and quality of X-ray data. X-ray data up to $(\sin\theta/\lambda)_{max} = 1.51$ Å^{-1} are now measured even for organic crystals using synchrotron radiations.[63] For extended structures, the maximum resolution of $(\sin\theta/\lambda)_{max} = 1.67$ Å^{-1} has been reported from single-crystal XRD of $CoSb_3$,[85] whereas it is pushed beyond $(\sin\theta/\lambda)_{max} = 1.8$ Å^{-1} for SPXRD using an all-in-vacuum diffractometer.[92] These ultra-high-resolution data show a model deficiency in the standard HC model and it has been subsequently improved by the EHC model.[97] The joint refinement of charge and spin densities by a combination of X-ray and neutron-diffraction data shows a recent advancement in the field. This unified method provides more detailed information on the spin-dependent EDD of magnetic crystals by obtaining complementary information from high-resolution X-ray data and polarized neutron-diffraction data. Likewise, complementary information available from XRD and NMR could be used for CD analysis. An empirical relationship between the Laplacian of the ED at the metal and the ^{1}H chemical shifts of agostic protons in planar d^8 transition metal complexes is shown in the study of agostic interactions.[120] There is also a possibility of using spin-density information from NMR measurements, but no such studies have been performed based on NMR data. A steady increase in the quality and resolution of X-ray data by latest technologies and synchrotron facilities might provide a new direction to CD research in the future.

Acknowledgement

I thank Prof. Eiji Nishibori, Prof. Bo B. Iversen and the University of Tsukuba for research facilities and funding.

Received: 14 February 2017 Accepted: 23 February 2017
Published online: 22 May 2017

References

1. Bragg WH (1921) The intensity of X-ray reflection by diamond. Proc Phys Soc (Lond) 33:304–311
2. Stewart RF (1976) Electron population analysis with rigid pseudo-atoms. Acta Crystallogr A 32:565–574
3. Hirshfeld FL (1976) Can X-ray data distinguish bonding effects from vibrational smearing. Acta Crystallogr A 32:239–244
4. Hansen NK, Coppens P (1978) Testing aspherical atom refinements on small-molecule datasets. Acta Crystallogr A 34:909–921
5. Bader RFW (1990) Atoms in molecules-A Quantum Theory. Clarendon, Oxford
6. Macchi P, Gillet JM, Taulelle F, Campo J, Claiser N, Lecomte C (2015) Modelling the experimental electron density: only the synergy of various approaches can tackle the new challenges. IUCrJ 2:441–451
7. Jorgensen MRV, Hathwar VR, Bindzus N, Wahlberg N, Chen YS, Overgaard J, Iversen BB (2014) Contemporary X-ray electron-density studies using synchrotron radiation. IUCrJ 1:267–280
8. Schmokel MS, Overgaard J, Iversen BB (2013) Experimental electron density studies of inorganic materials. Z Anorg Allg Chem 639:1922–1932
9. Dittrich B, Matta CF (2014) Contributions of charge-density research to medicinal chemistry. IUCrJ 1:457–469
10. Koritsanszky TS, Coppens P (2001) Chemical applications of X-ray charge-density analysis. Chem Rev 101:1583–1627
11. Gatti C (2005) Chemical bonding in crystals: new directions. Z Kristallogr 220:399–457
12. Stalke D (2011) Meaningful structural descriptors from charge density. Chem Eur J 17:9264–9278
13. Chopra D (2012) Advances in understanding of chemical bonding: inputs from experimental and theoretical charge density analysis. J Phys Chem A 116:9791–9801
14. Macchi P (2013) Modern charge density studies: the entanglement of experiment and theory. Crystallogr Rev 19:58–101
15. Krawczuk A, Macchi P (2014) Charge density analysis for crystal engineering. Chem Cent J 8:68
16. Coppens P (1997) X-ray charge densities and chemical bonding. Oxford University Press, Oxford
17. Tsirel'son VG, Ozerov RP (1996) Electron density and bonding in crystals. Institute of Physics Publishing, Bristol
18. Gatti C, Macchi P (2012) Modern charge density analysis. Springer, New York
19. Stalke D (2012) Electron density and chemical bonding I and II. Springer, Berlin Heidelberg
20. Friedrich W, Knipping P, von Laue M (1912) Interferenz-Erscheinungen bei Röntgenstrahlen, Sitzungsberichte der Kgl. Bayer. Akad. der Wiss, pp 303–322

21. Patterson AL (1934) A Fourier series method for the determination of the components of interatomic distances in crystals. Phys Rev 46:0372–0376
22. Karle J, Karle IL (1966) Symbolic addition procedure for phase determination for centrosymmetric and noncentrosymmetric crystals. Acta Crystallogr 21:849–859
23. Sayre D (1952) Some implications of a theorem due to Shannon. Acta Crystallogr 5:843
24. Dawson B (1967) Covalent bond in diamond. Proc R Soc Lond Ser A 298:264–288
25. Kurki-Suonio K (1968) On the information about deformations of the atoms in X-ray diffraction data. Acta Crystallogr A 24:379–390
26. Hishfeld FL (1971) Difference densities by least-squares refinement: fumaramic acid. Acta Crystallogr B 27:769–781
27. Coppens P, Row TNG, Leung P, Stevens ED, Becker PJ, Yang YW (1979) Net atomic charges and molecular dipole-moments from spherical-atom X-ray refinements, and the relation between atomic charge and shape. Acta Crystallogr A 35:63–72
28. Stewart RF (1977) One-electron density functions and many-centered finite multipole expansions. Isr J Chem 16:124–131
29. Hirshfeld FL (1976) Can X-ray data distinguish bonding effects from vibrational smearing. Acta Crystallogr A 32:239–244
30. Herbst-Irmer R, Henn J, Holstein JJ, Hubschle CB, Dittrich B, Stern D, Kratzert D, Stalke D (2013) Anharmonic motion in experimental charge density investigations. J Phys Chem A 117:633–641
31. Meindl K, Henn J (2008) Foundations of residual-density analysis. Acta Cryst A 64:404–418
32. Madsen AØ (2006) SHADE web server for estimation of hydrogen anisotropic displacement parameters. J Appl Cryst 39:757–758
33. Capelli SC, Burgi HB, Dittrich B, Grabowsky S, Jayatilaka D (2014) Hirshfeld atom refinement. IUCrJ 1:361–379
34. Jayatilaka D (1998) Wavefunction for beryllium from X-ray diffraction data. Phys Rev Lett 80:798–801
35. Checinska L, Morgenroth W, Paulmann C, Jayatilaka D, Dottrich B (2013) A comparison of electron density from Hirshfeld-atom refinement, X-ray wavefunction refinement and multipole refinement on three urea derivatives. Cryst Eng Comm 15:2084–2090
36. Guillot B, Viry L, Guillot R, Lecomte C, Jelsch C (2001) Refinement of proteins at subatomic resolution with MOPRO. J Appl Crystallogr 34:214–223
37. Volkov A, Macchi P, Farrugia LJ, Gatti C, Mallinson P, Richter T, Koritsanszky T (2016) XD2016—a computer program package for multipole refinement, topological analysis of charge densities and evaluation of intermolecular energies from experimental or theoretical structure factors
38. Becke AD, Edgecombe KE (1990) A simple measure of electron localization in atomic and molecular-systems. J Chem Phys 92:5397–5403
39. Bader RFW, Gatti C (1998) A Green's function for the density. Chem Phys Lett 287:233–238
40. Matta CF, Hernandez-Trujillo J, Tang TH, Bader RFW (2003) Hydrogen-hydrogen bonding: a stabilizing interaction in molecules and crystals. Chem Eur J 9:1940–1951
41. Kohout M (2004) A measure of electron localizability. Int J Quantum Chem 97:651–658
42. Johnson ER, Keinan S, Mori-Sanchez P, Contreras-Garcia J, Cohen AJ, Yang WT (2010) Revealing noncovalent interactions. J Am Chem Soc 132:6498–6506
43. Krawczuk A, Pérez D, Stadnicka K, Macchi P (2011) Distributed atomic polarizabilities from electron density. 1. Motivations and theory. Trans Am Crystallogr Assoc 42:1
44. Schleyer PV, Maerker C, Dransfeld A, Jiao HJ, Hommes NJRV (1996) Nucleus-independent chemical shifts: a simple and efficient aromaticity probe. J Am Chem Soc 118:6317–6318
45. Krawczuk A, Perez D, Macchi P (2014) PolaBer: a program to calculate and visualize distributed atomic polarizabilities based on electron density partitioning. J Appl Crystallogr 47:1452–1458
46. Saleh G, Lo Presti L, Gatti C, Ceresoli D (2013) NCImilano: an electron-density-based code for the study of noncovalent interactions. J Appl Crystallogr 46:1513–1517
47. Saleh G, Gatti C, Lo L (2015) Presti, Energetics of noncovalent interactions from electron and energy density distributions. Comput Theor Chem 1053:53–59
48. Koch U, Popelier PLA (1995) Characterization of C-H-O hydrogen-bonds on the basis of the charge-density. J Phys Chem 99:9747–9754
49. Overgaard J, Schiøtt B, Larsen FK, Iversen BB (2001) The charge density distribution in a model compound of the catalytic triad in serine proteases. Chem Eur J 7:3756–3767
50. Zhurov VV, Pinkerton AA (2015) Inter- and intramolecular interactions in crystalline 2-nitrobenzoic acid—an experimental and theoretical QTAIM analysis. J Phys Chem A 119:13092–13100
51. Bui TTT, Dahaoui S, Lecomte C, Desiraju GR, Espinosa E (2009) The nature of halogen···halogen interactions: a model derived from experimental charge-density analysis. Angew Chem Int Edit 48:3838–3841
52. Hathwar VR, Row TNG (2010) Nature of Cl···Cl intermolecular interactions via experimental and theoretical charge density analysis: Correlation of polar flattening effects with geometry. J Phys Chem A 114:13434–13441
53. Vener MV, Shishkina AV, Rykounov AA, Tsirelson VG (2013) Cl···Cl interactions in molecular crystals: Insights from the theoretical charge density analysis. J. Phys. Chem. A. 117:8459–8467

54. Chopra D, Row TNG (2011) Role of organic fluorine in crystal engineering. Cryst Eng Comm 13:2175–2186
55. Pavan MS, Prasad KD, Row TNG (2013) Halogen bonding in fluorine: experimental charge density study on intermolecular F···F and F···S donor-acceptor contacts. Chem Commun 49:7558–7560
56. Hathwar VR, Chopra D, Panini P, Row TNG (2014) Revealing the polarizability of organic fluorine in the trifluoromethyl group: implications in supramolecular chemistry. Cryst Growth Des 14:5366–5369
57. Dey D, Bhandary S, Sirohiwal A, Hathwar VR, Chopra D (2016) "Conformational lock" via unusual intramolecular C–F···O=C and C–H···Cl–C parallel dipoles observed in in–situ cryocrystallized liquids. Chem Commun 52:7225–7228
58. Mani D, Arunan E (2013) The X–C···Y (X = O/F, Y = O/S/F/Cl/Br/N/P) 'carbon bond' and hydrophobic interactions. Phys Chem Chem Phys 15:14377–14383
59. Thomas SP, Pavan MS, Row TNG (2014) Experimental evidence for 'carbon bonding' in the solid state from charge density analysis. Chem Commun 50:49–51
60. Thomas SP, Veccham SPKP, Farrugia LJ, Row TNG (2015) "Conformational simulation" of sulfamethizole by molecular complexation and insights from charge density analysis: role of intramolecular S···O chalcogen bonding. Cryst Growth Des 15:2110–2118
61. Sarkar S, Pavan MS, Row TNG (2015) Experimental validation of 'pnicogen bonding' in nitrogen by charge density analysis. Phys Chem Chem Phys 17:2330–2334
62. Pal R, Nagendra G, Samarasimhareddy M, Sureshbabu VV, Row TNG (2015) Observation of a reversible isomorphous phase transition and an interplay of "σ-holes" and "ϖ-holes" in Fmoc-Leu-Ψ[CH2-NCS]. Chem Commun 51:933–936
63. Hathwar VR, Sist M, Jorgensen MRV, Mamakhel AH, Wang XP, Hoffmann CM, Sugimoto K, Overgaard J, Iversen BB (2015) Quantitative analysis of intermolecular interactions in orthorhombic rubrene. IUCrJ 2:563–574
64. Hathwar VR, Thomsen MK, Mamakhel MAH, Filso MO, Overgaard J, Iversen BB (2016) Electron density analysis of the "O–O" charge-shift bonding in rubrene endoperoxide. J Phys Chem A 120:7510–7518
65. Sarkar S, Pavan MS, Cherukuvada S, Row TNG (2016) Acetazolamide polymorphism: a case of hybridization induced polymorphism? Chem Commun 52:5820–5823
66. Sovago I, Gutmann MJ, Hill JG, Senn HM, Thomas LH, Wilson CC, Farrugia LJ (2014) Experimental electron density and neutron diffraction studies on the polymorphs of sulfathiazole. Cryst Growth Des 14:1227–1239
67. Spackman MA (2015) How reliable are intermolecular interaction energies estimated from topological analysis of experimental electron densities? Cryst Growth Des 15:5624–5628
68. Espinosa E, Molins E, Lecomte C (1998) Hydrogen bond strengths revealed by topological analyses of experimentally observed electron densities. Chem Phys Lett 285:170–173
69. Wolff SK, Grimwood DJ, McKinnon JJ, Turner MJ, Jayatilaka D, Spackman MA (2015) CrystalExplorer 3.2. University of Western Australia, Perth
70. Woinska M, Jayatilaka D, Spackman MA, Edwards AJ, Dominiak PM, Wozniak K, Nishibori E, Sugimoto K, Grabowsky S (2014) Hirshfeld atom refinement for modelling strong hydrogen bonds. Acta Crystallogr A 70:483–498
71. Woińska M, Grabowsky S, Dominiak PM, Woźniak K, Jayatilaka D (2016) Hydrogen atoms can be located accurately and precisely by X-ray crystallography. Sci Adv 2:e1600192
72. Hirano Y, Takeda K, Miki K (2016) Charge-density analysis of an iron-sulfur protein at an ultra-high resolution of 0.48Å. Nature 534:281–284
73. Zarychta B, Lyubimov A, Ahmed M, Munshi P, Guillot B, Vrielink A, Jelsch C (2015) Cholesterol oxidase: ultra-high resolution crystal structure and multipolar atom model based analysis. Acta Crystallogr. D 71:954–968
74. Overgaard J, Walsh JPS, Hathwar VR, Jorgensen MRV, Hoffinan C, Platts JA, Piltz R, Winpenny REP (2014) Relationships between electron density and magnetic properties in water-bridged dimetal complexes. Inorg Chem 53:11531–11539
75. Dos Santos LHR, Lanza A, Barton AM, Brambleby J, Blackmore WJA, Goddard PA, Xiao F, Williams RC, Lancaster T, Pratt FL, Blundell SJ, Singleton J, Manson JL, Macchi P (2016) Experimental and theoretical electron density analysis of copper pyrazine nitrate quasi-low-dimensional quantum magnets. J Am Chem Soc 138:2280–2291
76. Wu LC, Weng TC, Hsu IJ, Liu YH, Lee GH, Jyh-Fu L, Wang Y (2013) Chemical bond characterization of a mixed-valence tri-cobalt complex, Co3(μ-admtrz)4(μ-OH)2(CN)6.2H2O. Inorg Chem 52:11023–11033
77. Deutsch M, Claiser N, Pillet S, Chumakov Y, Becker P, Gillet JM, Gillon B, Lecomte C, Souhassou M (2012) Experimental determination of spin-dependent electron density by joint refinement of X-ray and polarized neutron diffraction data. Acta Crystallogr A 68:675–686
78. Deutsch M, Gillon B, Claiser N, Gillet JM, Lecomte C, Souhassou M (2014) First spin-resolved electron distributions in crystals from combined polarized neutron and X-ray diffraction experiments. IUCrJ 1:194–199
79. Platts JA, Thomsen MK, Overgaard J (2013) Electron localisation in Ga-heterocyclic compounds. Z Anorg Allg Chem 639:1979–1984
80. Thomsen MK, Dange D, Jones C, Overgaard J (2015) Chemical bonding and electronic localization in a Ga^{I} amide. Chem Eur J 21:14460–14470
81. Scherer W, Meixner P, Barquera-Lozada JE, Hauf C, Obenhuber A, Bruck A, Wolstenholme DJ, Ruhland K,

Leusser D, Stalke D (2013) A unifying bonding concept for metal hydrosilane complexes. Angew Chem Int Edit 52:6092–6096

82. Scherer W, Dunbar AC, Barquera-Lozada JE, Schmitz D, Eickerling G, Kratzert D, Stalke D, Lanza A, Macchi P, Casati NPM, Ebad-Allah J, Kuntscher C (2015) Anagostic interactions under pressure: attractive or repulsive? Angew Chem Int Edit 54:2505–2509
83. Niepotter B, Herbst-Irmer R, Kratzert D, Samuel PP, Mondal KC, Roesky HW, Jerabek P, Frenking G, Stalke D (2014) Experimental charge density study of a silylone. Angew Chem Int Edit 53:2766–2770
84. Kratzert D, Leusser D, Holstein JJ, Dittrich B, Abersfelder K, Scheschkewitz D, Stalke D (2013) An experimental charge density study of two isomers of hexasilabenzene. Angew Chem Int Edit 52:4478–4482
85. Schmokel MS, Bjerg L, Larsen FK, Overgaard J, Cenedese S, Christensen M, Madsen GKH, Gatti C, Nishibori E, Sugimoto K, Takata M, Iversen BB (2013) Comparative study of X-ray charge-density data on $CoSb_3$. Acta Crystallogr A 69:570–582
86. Schmokel MS, Cenedese S, Overgaard J, Jorgensen MRV, Chen YS, Gatti C, Stalke D, Iversen BB (2012) Testing the concept of hypervalency: charge density analysis of K_2SO_4. Inorg Chem 51:8607–8616
87. Schmokel MS, Bjerg L, Cenedese S, Jorgensen MRV, Chen YS, Overgaard J, Iversen BB (2014) Atomic properties and chemical bonding in the pyrite and marcasite polymorphs of FeS_2: a combined experimental and theoretical electron density study. Chem. Sci. 5:1408–1421
88. Kurylyshyn IM, Fassler TF, Fischer A, Hauf C, Eickerling G, Presnitz M, Scherer W (2014) Probing the Zintl-Klemm concept: a combined experimental and theoretical charge density study of the Zintl phase CaSi. Angew Chem Int Edit 53:3029–3032
89. Eickerling G, Scherer W, Fickenscher T, Rodewald UC, Pottgen R (2013) Structure and chemical bonding of $ScNiB_4$. Z Anorg Allg Chem 639:2071–2076
90. Bindzus N, Straaso T, Wahlberg N, Becker J, Bjerg L, Lock N, Dippel AC, Iversen BB (2014) Experimental determination of core electron deformation in diamond. Acta Crystallogr A 70:39–48
91. Straaso T, Becker J, Iversen BB, Als-Nielsen J (2013) The Debye-Scherrer camera at synchrotron sources: a revisit. J Synchrotron Radiat 20:98–104
92. Wahlberg N, Bindzus N, Christensen S, Becker J, Dippel AC, Jorgensen MRV, Iversen BB (2016) Low-temperature powder X-ray diffraction measurements in vacuum: analysis of the thermal displacement of copper. J Appl Crystallogr 49:110–119
93. Nishibori E, Sunaoshi E, Yoshida A, Aoyagi S, Kato K, Takata M, Sakata M (2007) Accurate structure factors and experimental charge densities from synchrotron X-ray powder diffraction data at SPring-8. Acta Crystallogr A 63:43–52
94. Kastbjerg S, Bindzus N, Sondergaard M, Johnsen S, Lock N, Christensen M, Takata M, Spackman MA, Iversen BB (2013) Direct evidence of cation disorder in thermoelectric lead chalcogenides PbTe and PbS. Adv Funct Mater 23:5477–5483
95. Mondal S, Prathapa SJ, van Smaalen S (2012) Experimental dynamic electron densities of multipole models at different temperatures. Acta Crystallogr A 68:568–581
96. Svendsen H, Overgaard J, Busselez R, Arnaud B, Rabiller P, Kurita A, Nishibori E, Sakata M, Takata M, Iversen BB (2010) Multipole electron-density modelling of synchrotron powder diffraction data: the case of diamond. Acta Crystallogr A 66:458–469
97. Fischer A, Tiana D, Scherer W, Batke K, Eickerling G, Svendsen H, Bindzus N, Iversen BB (2011) Experimental and theoretical charge density studies at subatomic resolution. J Phys Chem A 115:13061–13071
98. Wahlberg N, Bindzus N, Bjerg L, Becker J, Dippel AC, Iversen BB (2016) Synchrotron powder diffraction of silicon: high-quality structure factors and electron density. Acta Crystallogr A 72:28–35
99. Wahlberg N, Bindzus N, Bjerg L, Becker J, Christensen S, Dippel AC, Jorgensen MRV, Iversen BB (2015) Powder X-ray diffraction electron density of cubic boron nitride. J Phys Chem C 119:6164–6173
100. Nishibori E, Shibata T, Kobayashi W, Moritomo Y (2015) Bonding nature of $LiCoO_2$ by topological analysis of electron density from X-ray diffraction. Electrochemistry 83:840–842
101. Guillot R, Fertey P, Hansen NK, Alle P, Elkaim E, Lecomte C (2004) Diffraction study of the piezoelectric properties of low quartz. Eur Phys J B 42:373–380
102. Fertey P, Alle P, Wenger E, Dinkespiler B, Cambon O, Haines J, Hustache S, Medjoubi K, Picca F, Dawiec A, Breugnon P, Delpierre P, Mazzoli C, Lecomte C (2013) Diffraction studies under in situ electric field using a large-area hybrid pixel XPAD detector. J Appl Crystallogr 46:1151–1161
103. Pillet S, Legrand V, Weber HP, Souhassou M, Letard JF, Guionneau P, Lecomte C (2008) Out-of-equilibrium charge density distribution of spin crossover complexes from steady-state photocrystallographic measurements: experimental methodology and results. Z Kristallogr 223:235–249
104. Katrusiak A (2008) High-pressure crystallography. Acta Crystallogr A 64:135–148
105. Aoyagi S, Toda S, Nishibori E, Kuroiwa Y, Ohishi Y, Takata M, Sakata M (2008) Charge density distribution of $KMnF_3$ under high pressure. Phys Rev B 78:224102
106. Casati N, Kleppe A, Jephcoat AP, Macchi P (2016) Putting pressure on aromaticity along with in situ experimental electron density of a molecular crystal. Nat Commun 7:10901

107. Munshi P, Row TNG (2005) Exploring the lower limit in hydrogen bonds: analysis of weak C-H···O and C–H···ϖ interactions in substituted coumarins from charge density analysis. J Phys Chem A 109:659–672
108. Munshi P, Row TNG (2005) Charge density based classification of intermolecular interactions in molecular crystals. Cryst Eng Comm 7:608–611
109. Chopra D, Cameron TS, Ferrara JD, Row TNG (2006) Pointers toward the occurrence of C-F···F–C interaction: experimental charge density analysis of 1-(4-Fluorophenyl)-3,6,6-Trimethyl-2-phenyl-1,5,6,7-Tetrahydro-4H-indol-4-one and 1-(4-Fluorophenyl)-6-Methoxy-2-phenyl-1,2,3,4-Tetrahydroisoquinoline. J Phys Chem A 110:10465–10477
110. Hathwar VR, Gonnade RG, Munshi P, Bhadbhade MM, Row TNG (2011) Halogen bonding in 2,5-dichloro-1,4-benzoquinone: insights from experimental and theoretical charge density analysis. Cryst Growth Des 11:1855–1862
111. Hathwar VR, Row TNG (2011) Charge density analysis of heterohalogen (Cl···F) and homohalogen (F···F) intermolecular interactions. Cryst Growth Des 11:1338–1346
112. Hathwar VR, Thakur TS, Row TNG, Desiraju GR (2011) Transferability of multipole charge density parameters for supramolecular synthons: a new tool for quantitative crystal engineering. Cryst Growth Des 11:616–623
113. Hathwar VR, Thakur TS, Dubey R, Pavan MS, Row TNG, Desiraju GR (2011) Extending the supramolecular synthon based fragment approach (SBFA) for transferability of multipole charge density parameters to monofluorobenzoic acids and their cocrystals with isonicotinamide: importance of C–H···O, C–H···F, and F···F intermolecular regions. J Phys Chem A 115:12852–12863
114. Kulkarni GU, Kumaradhas P, Rao CNR (1998) Charge density study of the polymorphs of p-nitrophenol. Chem Mater 10:3498–3505
115. Gopalan RS, Kulkarni GU, Rao CNR (2000) An experimental charge density study of the effect of the noncentric crystal field on the molecular properties of organic NLO materials. Chem Phys Chem 1:127–135
116. Kumar A, Gadre SR (2016) Exploring the gradient paths and zero flux surfaces of molecular electrostatic potential. J Chem Theory Comput 12:1705–1713
117. Kumar A, Gadre SR, Mohan N, Suresh CH (2014) Lone pairs: an electrostatic viewpoint. J Phys Chem A 118:526–532
118. Balanarayan P, Gadre SR (2006) Atoms-in-molecules in momentum space: a Hirshfeld partitioning of electron momentum densities. J Chem Phys 124:204113
119. Kumar A, Yeole SD, Gadre SR, Lopez R, Rico JF, Ramirez G, Ema I, Zorrilla D (2015) DAMQT 2.1.0: a new version of the DAMQT package enabled with the topographical analysis of electron density and electrostatic potential in molecules. J Comput Chem 36:2350–2359
120. Barquera-Lozada JE, Obenhuber A, Hauf C, Scherer W (2013) On the chemical shifts of agostic protons. J Phys Chem A 117:4304–4315

Venkatesha R. Hathwar is Assistant Professor at the Faculty of Pure and Applied Sciences, University of Tsukuba, Japan, since May 2016. He was born in Udupi, Karnataka and received his B.Sc. and M.Sc. degrees from S.D.M. College, Ujire, Karnataka and Mangalore University, Mangalore, Karnataka, respectively. He completed his Ph.D. from the Indian Institute of Science with Prof. T.N. Guru Row in 2011. It was followed by two postdoctoral research works at the University of Augsburg, Germany, with Prof. Wolfgang Scherer and at Aarhus University, Denmark with Prof. Bo B. Iversen. He is also the recipient of AsCA Rising Star Award in 2009 from the Asian Crystallographic Association. His current research interests include synthesis of functional materials, electron density studies, high-pressure crystallography, and synchrotron X-ray diffraction.